SCANNING VOL. 9999, 1–10 (2016)
© Wiley Periodicals, Inc.

Atomic Force Microscopy Study of Ionomycin-Induced Degranulation in RBL-2H3 Cells

Jiang Pi,[1] Lufen Huang,[1] Fen Yang,[1] Jinhuan Jiang,[1] Hua Jin,[1] Jianxin Liu,[1,2] Xiaohui Su,[1] Anguo Wu,[1] Huaihong Cai,[3] Peihui Yang,[2] and Jiye Cai[1,3]

[1]State Key Laboratory of Quality Research in Chinese Medicines, Macau University of Science and Technology, Macau, China
[2]Department of Pharmacology, Hunan University of Medicine, Huaihua, China
[3]Department of Chemistry, Jinan University, Guangzhou, China

Summary: Mast cell degranulation is the typical anaphylaxis process of mast cells associated with the release of cytokines, eicosanoids and their secretory granules, which play very important roles in the allergic inflammatory response of the human body upon anaphylactogen stimulation. The calcium ionophore ionomycin is widely used as a degranulation induction agent for mast cell degranulation studies. In the present work, ionomycin-induced degranulation of RBL-2H3 basophilic leukemia cell line cells was investigated *in vitro* by high resolution atomic force microscopy (AFM). Ionomycin, which could increase the intracellular free Ca^{2+} level and β-Hexosaminidase release, was found to induce the formation of a kind of peculiar vesicles in the cytoplasm area of RBL-2H3 cells. Those vesicles induced by ionomycin would desintegrate to release a larger amount of granules surrounding RBL-2H3 cells by the controlling of F-actin. These results provide the precise morphological information of ionomycin-induced mast cell degranulation at nanoscale, which could benefit our understanding of ionomycin-induced mast cell anaphylaxis model and also validate the applicability of AFM for the detection of allergic inflammatory response in mast cells. SCANNING 9999:1–10, 2016. © Wiley Periodicals, Inc.

Key words: ionomycin, mast cells, degranulation, atomic force microscopy

Introduction

Anaphylaxis, a severe systemic allergic response, which is rapid at onset and potentially lethal, is typically induced by an innocuous substance. Anaphylaxis occurs rapidly and systemically, typically involves the cutaneous, respiratory, cardiovascular, and gastrointestinal systems, targeting organs heavily populated with mast cells (Sampson *et al*., 2005). Anaphylaxis is always caused by the exposure of allergen or other factors, which activate mast cells or basophils, prompt the degranulation and immediate release of preformed inflammation mediators (such as histamine, β-Hexosaminidase, tryptase, carboxypeptidase A, and proteoglycans), induce the synthesis of arachidonic acid metabolites (prostaglandins, leukotrienes) and the generation of cytokines (TNF-α) and chemokines (Metcalfe *et al*., 2009).

Mast cells, a kind of cells derived from myeloid stem cells and contain many granules inside the cells, are thought to be intimately involved in wound healing and immunity defense against pathogens (Stone *et al*., 2010). But the main function of mast cells is their roles in anaphylaxis, which are the central events in allergic diseases (Metcalfe *et al*., 2009). Mast cells have important impacts on the initiation and development of allergic response, which can be activated by a series of stimuli (Kemp and Lockey, 2002; Lenchner and Grammer, 2003), mainly through IgE (FcRI)-dependent or independent mechanisms. The investigation of mast cell activation could not only contribute to our understanding of anaphylaxis processes, but also lead to the discovery of novel therapeutic targets for

Contract grant sponsor: Macao Science and Technology Development; Contract grant number: 028/2014/A1; Contract grant sponsor: Overseas, Hong Kong & Macao Cooperative Research; Contract grant number: 31129002; Contract grant sponsor: Jinan University's Scientific Research Cultivation and Innovation; Contract grant number: 21612601.

Jiang Pi and Lufen Huang contributed equally to this paper and share the first authorship.

Address for reprints: Jiye Cai, State Key Laboratory of Quality Research in Chinese Medicines, Macau University of Science and Technology, Macau 000853, China.
E-mail: tjycai@jnu.edu.cn

Received 2 October 2015; Accepted with revision 22 November 2015

DOI: 10.1002/sca.21291
Published online XX Month Year in Wiley Online Library (wileyonlinelibrary.com).

anaphylaxis treatment, which make mast cell a best suitable candidate for anaphylaxis studies. Ionomycin, produced by the bacterium Streptomyces Conglobatus, is a mobile ion carrier for Ca^{2+} that widely used to study the effects of calcium flux on endoplasmic reticulum (ER) stress, mitochondrial stress and intrinsic apoptosis mechanisms (Giannone *et al*., 2004; Liu *et al*., 2012). Otherwise, ionomycin is also an anaphylaxis induction agent by inducing mast cell degranulation, which provides a different degranulation mechanism compared with the traditional lgE-mediated mast cell degranulation (Shumilina *et al*., 2008; Kraft *et al*., 2013). But up to now, the exact degranulation mechanism of mast cells induced by ionomycin is still poorly understood.

Techniques used for mast cell degranulation studies always focus on the biochemical response of mast cells upon external stimulation, such as the β-hexosaminidase release assay (Schwartz *et al*., '79; Mastuda *et al*., 2002) and histamine release assay (Je *et al*., 2015). Unlike these biomedical analysis assays, microscopy studies could provide more direct morphological information of cells during cell signaling processes, such as mast cell degranulation. Conventional light microcopies could image mast degranulation with whole cell morphological information, but the precise morphological information is still limited due to its diffraction limit. Thus, some high resolution microscopies, such as scanning electron microscopy (Urb *et al*., 2009) and transmission electron microscopy (Zhang *et al*., 2011) were also applied for mast cell degranulation studies, which could provide more precise information of the degranulation processes. However, despite the long-term and harmful sample preparation procedures, transmission electron microscopy could just image intracellular structures, which could just provide the intracellular structure changes during the granulation processes. Scanning electron microscopy, could provide the extracellular or membrane- associated behavior during mast cell degranulation, but the complicated sample preparation procedures, such as the long time fixation, dehydration, dry and evaporative deposition procedures, are very harmful to the cell sample, which might influence the detection result.

As a member of scanning probe microscopy (SPM) techniques, atomic force microscopy (AFM) permits the observation of biological samples ranging from single molecule to tissue because of its pico-newton sensitivity and nanometer spatial resolution. Relying on the detection of cantilever deflection induced by the forces between the AFM tip and sample, AFM has become one of the most powerful nanotechniques for *in situ* single molecule detection of cells, especially for *in situ* single molecule imaging on/in cell membranes (Pi *et al*., 2014a). Besides, AFM is also a convenient and fast-detecting technique for high resolution cellular morphology imaging and for sensitive cellular biomechanical property determination (Dupres *et al*., 2005; Lekka and Laidler, 2009; Pi *et al*., 2014b). And the sample preparation procedures for AFM imaging are also much simpler than that of scanning electron microscopy and transmission electron microscopy, which could reflect the cell behaviors more veritably. Based on these properties, AFM has also been introduced for the study of mast cells in recent years, providing some important information of mast cell activation at nanoscale (Ohshiro *et al*., 2000; Frankel *et al*., 2006; Hu *et al*., 2014). The degranulation process of rat peritoneal mast cells was visualized by AFM, which showed the secretory granules packed in the cytoplasm by high resolution imaging (Nakamura and Nakanishi, '99). The effects of immune-receptor tyrosine-based activation motifs-bearing FcγRIIB2 on the FcRI-dependent activation of rat basophilic leukemia (RBL-2H3) cells had also been investigated by AFM, which suggested that mast cell secretory responses triggered by high-affinity receptor for IgE might be controlled by low-affinity receptors for IgG (Nakamura and Nakanishi, 2000).

In the present work, we investigated the degranulation processes of control RBL-2H3 cells and ionomycin-treated RBL-2H3 cells by high resolution AFM. These results obtained at nanoscale demonstrated a different degranulation way between ionomycin-stimulated RBL-2H3 cells and control RBL-2H3 cells, which would benefit our understanding of mast cell anaphylaxis induced by ionomycin.

Materials and Methods

Materials

Ionomycin (Catalogue Number: I9657, Batch Number: 074M4030V), β-Hexosaminidase substrate solution (Catalogue Number: N9376, Batch Number: SLBF1695V) and paraformaldehyde (Catalogue Number: p6148, Batch Number: 091M1290V) were purchased from Sigma (Sigma-Aldrich, St. Louis, MO, USA). DMEM medium, trypsin and fetal bovine serum (FBS) were obtained from GIBCO (Gibco-Invitrogen, Carlsbad, CA, USA). Penicillin and streptomycin were purchased from Invitrogen (UK). FITC-phalloidin (Actin-tracker green, Catalogue Number: C1033) kit and Fluo-3 AM (calcium fluorescence probe, Catalogue Number: S1056) kit were obtained from Beyotime (China). All reagents used in the experiments were of analytical grade.

Cell Culture

RBL-2H3 cells were purchased from the American Type Culture Collection (American Type Culture Collection, USA), and cultured in DMEM medium supplemented with 10% FBS and 100 U/mL penicillin and 100 U/mL streptomycin at 5% CO_2 and 37°C in a humidified incubator.

Measurement of Intracellular Ca^{2+} Level

The intracellular Ca^{2+} level of RBL-2H3 cells was quantified by flow cytometry using Fluo-3 AM as fluorescence probe. RBL-2H3 cells seeded at a density of 2×10^6 cells/well in 6-well plates were stimulated with 10 μg/mL ionomycin for 5, 10, and 30 min, respectively. Cells were harvested with 0.25% trypsin, washed with PBS and incubated with 5 μM Fluo-3 AM for 30 min. After washed with PBS, cells were analyzed by flow cytometer using an excitation wavelength of 488 nm (BD, Franklin Lakes, NJ, USA).

Measurement of β-Hexosaminidase Release

Degranulation response of RBL-2H3 basophils was quantified by determining the level of released β-hexominedase in the supernatant. RBL-2H3 cells seeded at a density of 2×10^5 cells/well in 96-well plates were stimulated with 10 μg/mL ionomycin for 5, 10, and 30 min, respectively. The plate was then centrifuged at 1,000 rpm for 5 min and 30 μL supernatant from each well was transferred to another flat bottom plate for enzyme activity analysis. 20 μL of supernatants were mixed with 20 μL of substrate solution in 96-well plates and incubated for 1 h at 37˚C. The reaction was then terminated by the addition of 200 μL of 0.2 M Glycine (pH 10.7). Absorbance was measured at 405 nm (TECAN, Männedorf, Switzerland). The results of cell degranulation were expressed as the percentage of degranulation in control sample.

F-Actin Structure Analysis

The structure of F-actin in RBL-2H3 cells was investigated by fluorescence microscopy using special staining of F-actin with actin-tracker green. RBL-2H3 cells were seeded onto a glass slide in 6-well plates at a density of 5×10^4 cells/well. After overnight incubation, cells were stimulated with 10 μg/mL ionomycin for 5, 10, and 30 min, respectively, washed with PBS and fixed by 4% paraformaldehyde for 10 min. After washed with PBS (1% Triton × 100), cells were then incubated with 200 μL FITC-phalloidin for 60 min in dark at room temperature. After washed triple with PBS, a fluorescence microscopy (Applied Precision, Canada) was used to image the organization of F-actin cytoskeleton structure.

AFM Imaging

RBL-2H3 cells were harvested with 0.25% trypsin and cultured at density of 5×10^4 cells/mL into 25 mm dishes. After overnight incubation, cells were directly stimulated with 10 μg/mL ionomycin for 5, 10, and 30 min, respectively. Cells were then washed triple with PBS, fixed with 4% paraformaldehyde solution for 10 min, washed triple with distilled water and dried in air for morphology imaging in air.

High resolution AFM (Bruker, German) was used to investigate ionomycin-induced cellular morphological and cell surface ultrastructural changes of RBL-2H3 cells. Silicon nitride tips (BudgetSensors, Bulgaria) used in all measurements were irradiated by ultraviolet to remove the organic contaminates. The curvature radius of the AFM tips used for morphology imaging is 10 nm, and the spring constant of tips is 1.35 ± 0.27 N/m with a deflection sensitivity of 14.23 ± 0.59 nm/V. The high resolution morphological images of RBL-2H3 cells were measured in air at room temperature in contact mode.

Statistical Analysis

All data presented are expressed as Mean ± S.E.M., and representative of three or more independent experiments. Statistical analysis was performed using Student's *t*-test, and $p < 0.05$ was regarded as statistically significant.

Results and Discussion

Effects of Ionomycin on Intracellular Ca^{2+} Level of RBL-2H3 Cells

RBL-2H3 cell line is a common histamine-releasing cell model used for inflammatory, allergic and immunological research (Passante *et al.*, 2009; Passante and Frankish, 2009). Ca^{2+}, a kind of ions necessary for the physiological activity of body (Clapham, 2007), also plays very important roles in mast cell functions (Neher, '88; Kempuraj *et al.*, 2005). Ionomycin is an ionophore, which can raise the intracellular level of Ca^{2+} and produce some inflammation dependent cytokines. The function of ionomycin in mast cells is closely associated with the intracellular Ca^{2+} level, as the inhibition of intracellular Ca^{2+} level increase can prevent ionomycin-induced mast cell degranulation (Hong *et al.*, 2011; Yang *et al.*, 2014). The effects of ionomycin on the intracellular Ca^{2+} level of RBL-2H3 cells were determined by flow cytometry analysis. As shown in Figure 1(A–D), ionomycin treatment could increase the intracellular Ca^{2+} level of RBL-2H3 cells immediately. The statistical results (Fig. 1(E)) demonstrated that the intracellular Ca^{2+} level of RBL-2H3 cells increased from $100.0 \pm 2.8\%$ (control cells) to $119.7 \pm 6.1\%$, $180.6 \pm 8.2\%$ and $222.4 \pm 2.0\%$ after 5, 10, and 30 min ionomycin stimulation, respectively. These results implied that ionomycin could induce Ca^{2+} influx in RBL-2H3 cells, which was reported to be

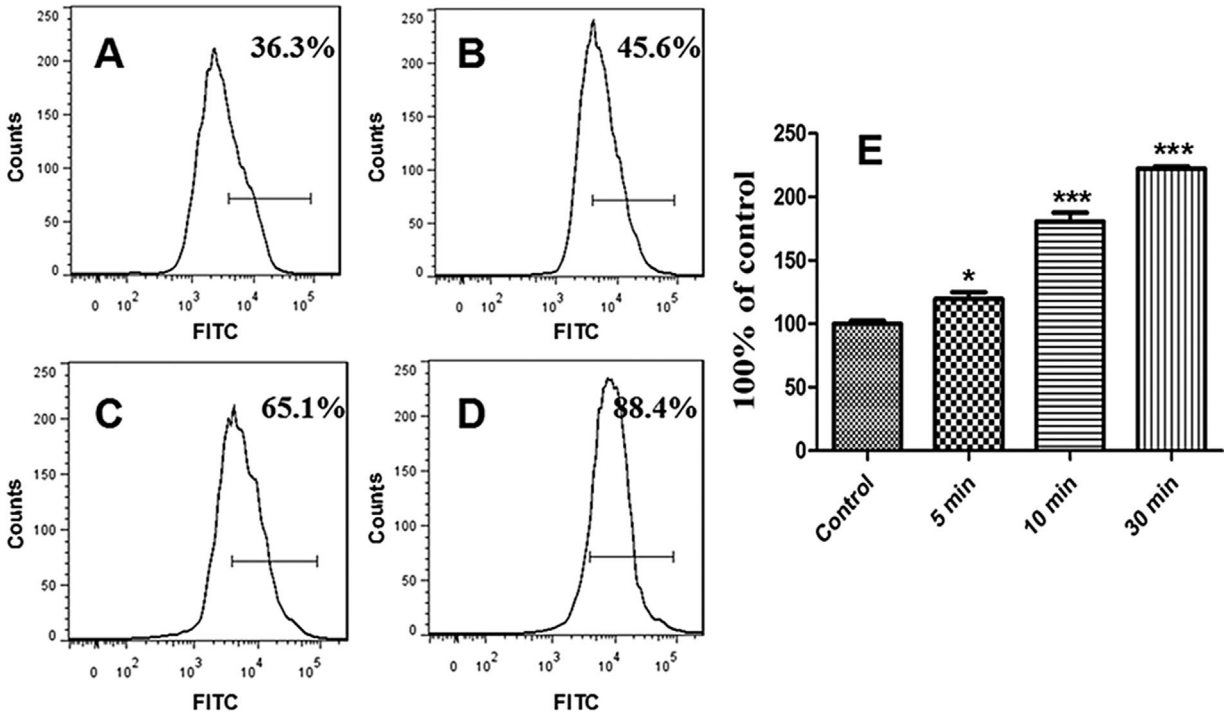

Fig 1. Effects of ionomycin on the intracellular Ca^{2+} level in RBL-2H3 cells determined by flow cytometry. (A) Control, (B) 5 min ionomycin stimulated, (C) 10 min ionomycin stimulated, and (D) 30 min ionomycin-stimulated RBL-2H3 cells. (E) Statistic results of the intracellular Ca^{2+} level in RBL-2H3 cells, $n = 6$ $^{*}p < 0.05$, $^{***}p < 0.001$.

important roles in the regulation of mast cell activation (Baba *et al*., 2008).

Effects of Ionomycin on β-Hexosaminidase Release in RBL-2H3 Cells

β-hexosaminidase, a kind of glucoside hydrolases, has been found to be released during mast cell degranulation and thus been widely used as biomarkers for the degranulation of mast cells (Schwartz *et al*., '79; Mastuda *et al*., 2002). To confirm the strong degranulation induction effects of ionomycin in mast cells, β-hexosaminidase level was examined in the supernatant of RBL-2H3 cells. As shown in Figure 2, β-hexosaminidase level in the supernatant of RBL-2H3 cells increased from $100.0 \pm 9.3\%$ for control cells to $631.8 \pm 48.1\%$, $1621.2 \pm 278.1\%$, and $2123.1 \pm 412.3\%$ after 5, 10, and 30 min ionomycin treatment, respectively. The increased level of β-hexosaminidase upon ionomycin stimulation indicated that ionomycin could significantly enhance the degranulation of RBL-2H3 cells.

AFM Imaging of the Granulation of Control RBL-2H3 Cells

The degranulation of RBL-2H3 cells has been studied by different microscopies to show their degranulation processes (Huang *et al*., 2010; Yang *et al*., 2010). But the limited resolution of light microscopy still restricts our understanding of the detailed degranulation processes of RBL-2H3 cells. Here, high resolution AFM was operated to investigate the detailed morphological changes of RBL-2H3 cells induced by ionomycin stimulation at nanometer scale. The typical topography, deflection error and corresponding 3-D images of control RBL-2H3 cells were shown in Figure 3. Control RBL-2H3 cells always presented as spindle or irregular shapes (Fig. 3). From AFM morphology imaging, the nucleus area and cytoplasm area could be identified because the nucleus area was much higher than cytoplasm area (Supplementary materials Fig. S1). Through high

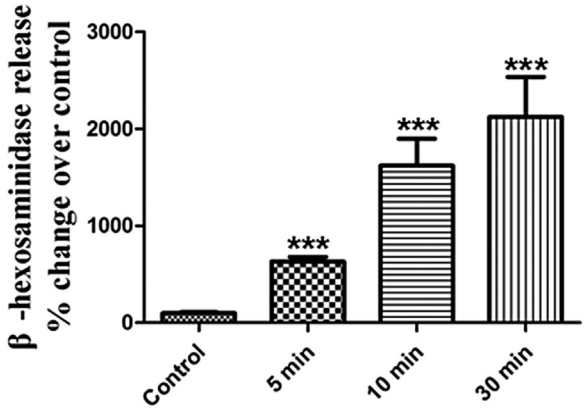

Fig 2. Effects of ionomycin on the release of β-hexosaminidase in RBL-2H3 cells, $n = 5$, $^{***}p < 0.001$.

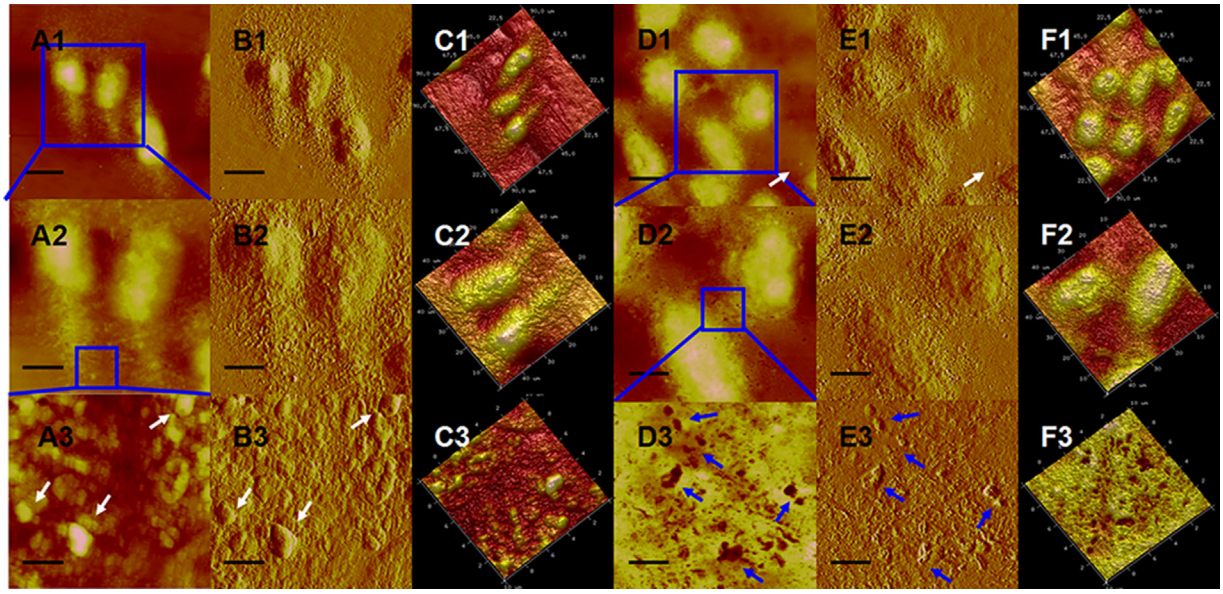

Fig 3. Morphology and ultrastructure of control RBL-2H3 cells determined by AFM. (A1-3, D1-3) Topography, (B1-3, E1-3) deflection error and (C1-3,F1-3) the corresponding 3D images of control RBL-2H3 cells. Scale bar in (A1-F1): 20 μm, scale bar in (A2-F2): 10 μm, and scale bar in (A3-F3): 2 μm. The white arrows indicate the location of granules and the blue arrows indicate the emergence of pores in the membrane of RBL-2H3 cells.

resolution cell membrane imaging, we could find some uneven sized granules (shown as white arrows in Fig. 3) and pores (shown as blue arrows in Fig. 3) located on the membrane of cytoplasm area. The granules observed on cell membrane, which were considered to be the granules intended for degranulation, showed diameters ranging from 200 to 2,000 nm and height ranging from 10 to 500 nm (Supplementary materials Fig. S 2). And the pores emerged on cell membrane, which were considered to be the invaginated membrane structure during degranulation, showed diameter distribution ranging from 300 to 5,000 nm and depth distribution ranging from 10 to 500 nm (Supplementary materials Fig. S 3). The average size of the granules and pores was also quantified by AFM analysis, which demonstrated that the average diameter and depth of the pores were 961.2 ± 47.4 nm and 129.1 ± 6.4 nm, respectively. And the average diameter and height of the granules were 1000.7 ± 58.4 nm and 71.1 ± 6.2 nm, respectively. It was also worth to note that most of the observed granules or pores were located in the cytoplasm area. These results suggested that the degranulation of control RBL-2H3 cells was mainly happened in the cytoplasm areas of RBL-2H3 cells. Ohashi *et al.* '94 also demonstrated the pores with average size at 600–800 nm and granules with average size of 600 nm on mast cells from mice by scanning electron microscopy, which were similar with the results we obtained by AFM imaging. Additionally, not all granules were released into the supernatant of RBL-2H3 cells, because granules could also be observed on the substrate, at the edge of RBL-2H3 cells (Supplementary materials Fig. S 5). All these results collectively suggested that degranulation was a common function of RBL-2H3 cells, which could be also found in control cells. Moreover, the degranulation of control RBL-2H3 cells were mainly happened in the cytoplasm area of cells and part of the released granules were absorbed onto the substrate.

AFM Imaging of the Granulation of Ionomycin-Stimulated RBL-2H3 Cells

Ionomycin was added into RBL-2H3 cells for 5 min stimulation to determine the effects of ionomycin on the early stage activation of mast cells. With ionomycin treatment, the shrinking cytoplasm area of RBL-2H3 cells could be found by AFM imaging (Fig. 4). Granules (shown as white arrows in Fig. 4) and pores (shown as blue arrows in Fig. 4) were also found in cytoplasm area of RBL-2H3 cells, indicating the similar degranulation way for RBL-2H3 cells in the early stage of ionomycin treatment.

After 10 min ionomycin stimulation, the shrinking of cytoplasm area became a more common case in RBL-2H3 cells (Fig. 5). And particularly, the formation of a kind of peculiar vesicles was found in RBL-2H3 cells after 10 min ionomycin treatment (shown as red arrows in Fig. 5). But these peculiar vesicles did not separate from the native cell bodies of RBL-2H3 cells immediately, which were still contacted with the cytoplasm of RBL-2H3 cells through some fibre-like structures (shown as green arrows in Fig. 5). Moreover, some granules could be observed in or around these peculiar vesicles by AFM imaging (shown as white arrows in Fig. 5(A3–E3)). Similar results were

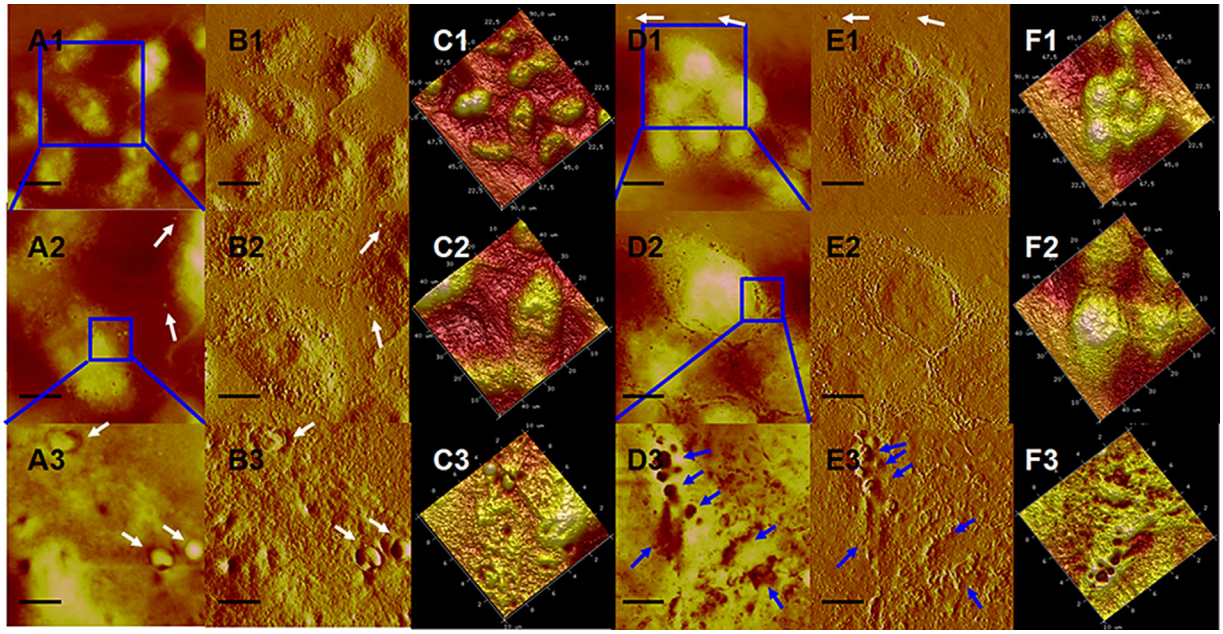

Fig 4. Morphology and ultrastructure of RBL-2H3 cells after 5 min ionomycin treatment determined by AFM. (A1-3, D1-3) Topography, (B1-3, E1-3) deflection error and (C1-3,F1-3) the corresponding 3D images of control RBL-2H3 cells. Scale bar in (A1-F1): 20 μm, scale bar in (A2-F2): 10 μm and scale bar in (A3-F3): 2 μm. The white arrows indicate the location of granules and the blue arrows indicate the emergence of pores in the membrane of RBL-2H3 cells.

also obtained in RBL-2H3 cells after 30 min treatment of ionomycin, which showed shrunk cytoplasm, formation of peculiar vesicles, and the location of granules in or around these peculiar vesicles (Fig. 6). Moreover, the peculiar vesicles induced by ionomycin seemed to disintegrate into smaller granules with 30 min ionomycin treatment (shown as white arrows in Fig. 6), and the fibre-like structures disappeared with the disintegration of the peculiar vesicles (Fig. 6(D–F)). These results collectively suggested that the peculiar vesicles seemed to play very important roles in ionomycin-induced degranulation of RBL-2H3 cells. The several micrometer sized vesicles protruded from the native cell body of RBL-2H3 cells (Fig. 7(A)) to

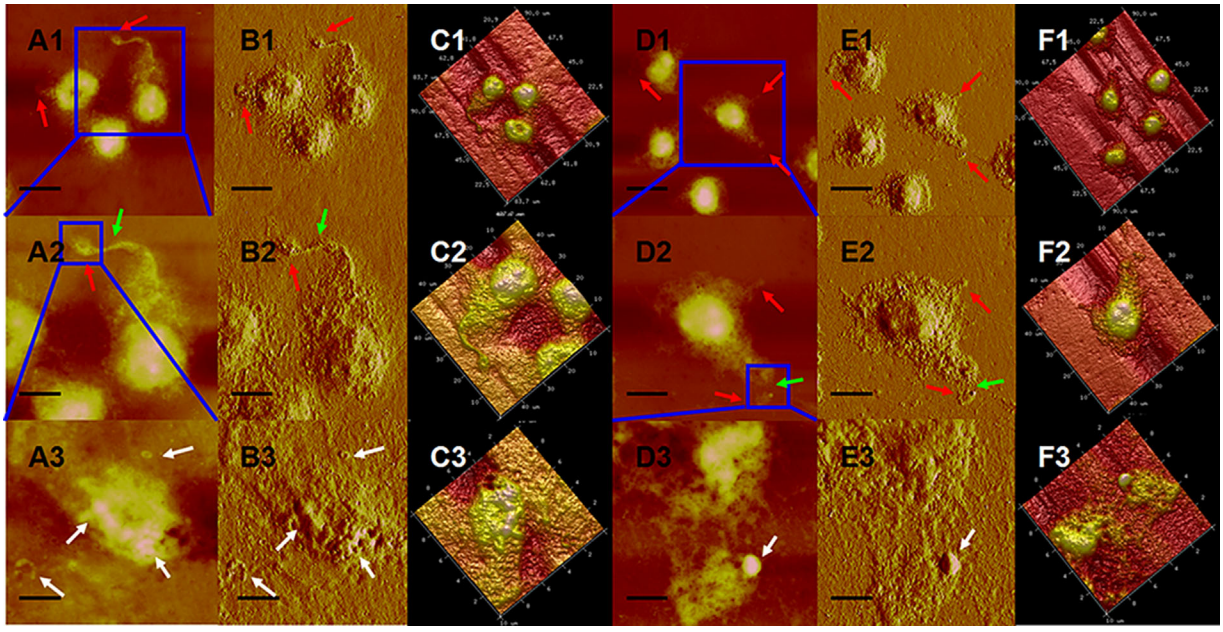

Fig 5. Morphology and ultrastructure of RBL-2H3 cells after 10 min ionomycin treatment determined by AFM. (A1-3, D1-3) Topography, (B1-3, E1-3) deflection error and (C1-3,F1-3) the corresponding 3D images of control RBL-2H3 cells. Scale bar in (A1-F1): 20 μm, scale bar in (A2-F2): 10 μm and scale bar in (A3-F3): 2 μm. The white arrows indicate the location of granules, the red arrows indicate the formation of unknown vesicles and the green arrows indicate the linker between the unknown vesicles and RBL-2H3 cells.

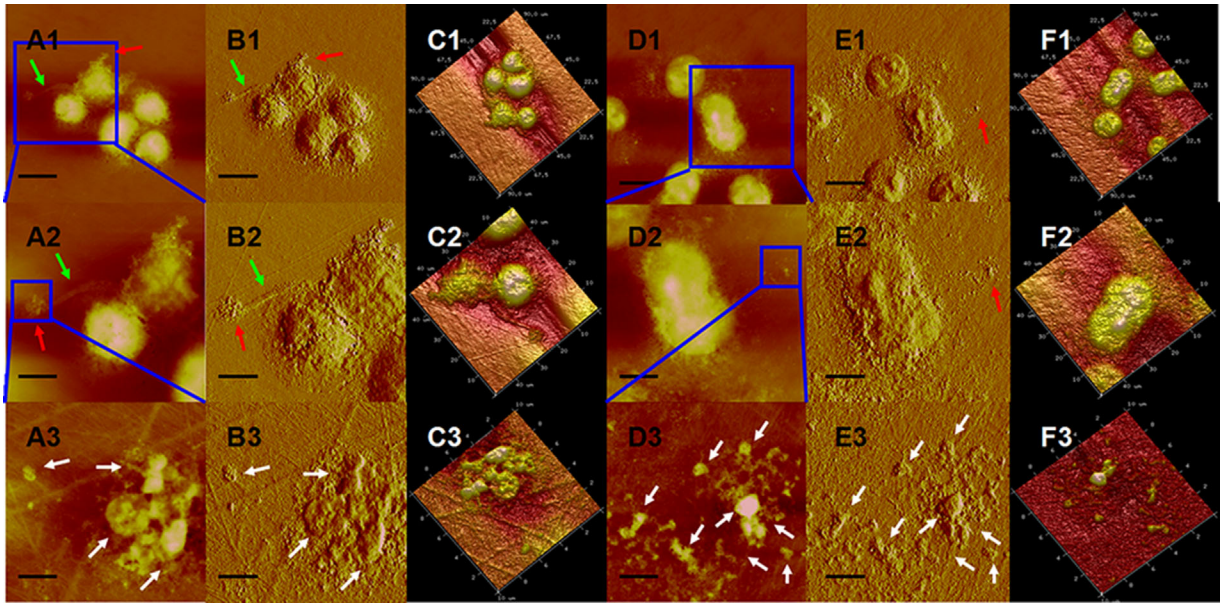

Fig 6. Morphology and ultrastructure of RBL-2H3 cells after 30 min ionomycin treatment determined by AFM. (A1-3, D1-3) Topography, (B1-3, E1-3) deflection error and (C1-3, F1-3) the corresponding 3D images of control RBL-2H3 cells. Scale bar in (A1-F1): 20 μm, scale bar in (A2-F2): 10 μm and scale bar in (A3-F3): 2 μm. The white arrows indicate the location of granules, the red arrows indicate the formation of unknown vesicles and the green arrows indicate the linker between the unknown vesicles and RBL-2H3 cells.

deviate from the cytoplasm of RBL-2H3 cells by fibre-like structures (Fig. 7(B)), which finally separated from the cytoplasm of RBL-2H3 cells (Fig. 7(C)). The cross line analysis indicated that the size distribution of the peculiar vesicles ranged from 1–10 μm and height distribution ranging from 50–300 nm (Fig. 7(A3–C3)). During this process, degranulation was observed in these peculiar vesicles to release different sized granules,

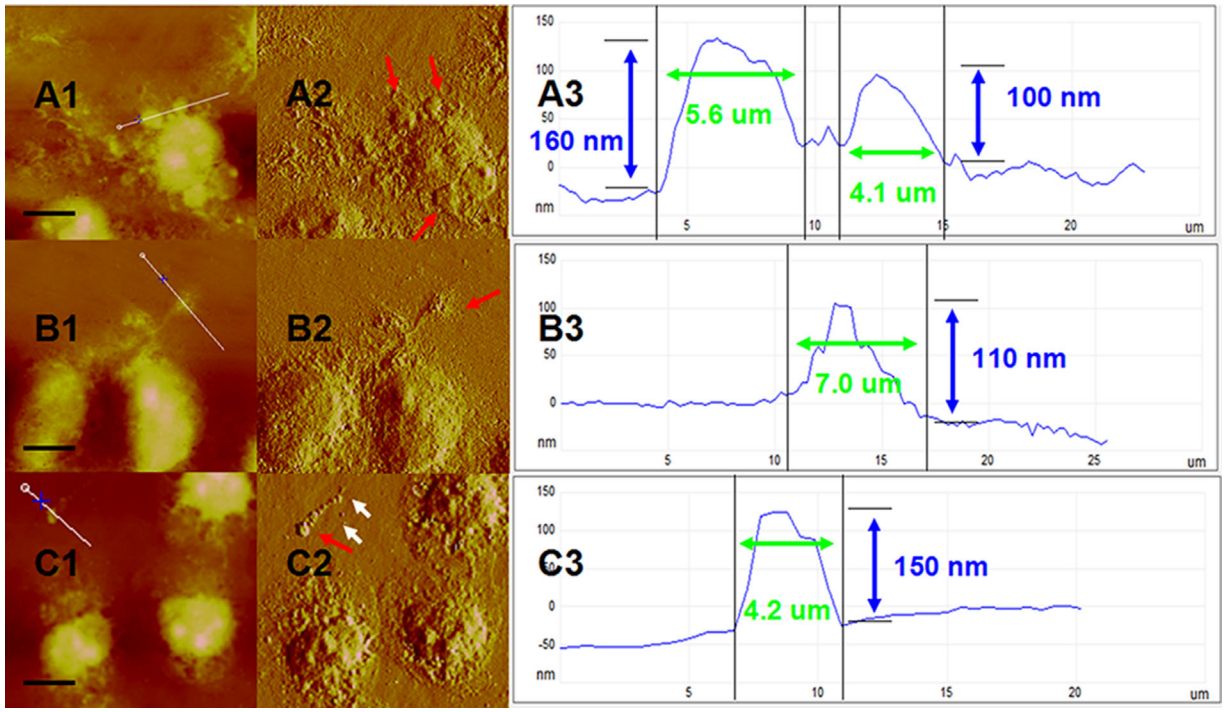

Fig 7. Formation of the unknown vesicles in RBL-2H3 cells induced by ionomycin. (A) Vesicles protruded from the native cell body of RBL-2H3 cells, (B) Vesicles connected with the native cell body of RBL-2H3 cells and (C) vesicles separated from the native cell body of RBL-2H3 cells. (A1-C1) Topography and (A2-C2) deflection error of RBL-2H3 cells, the red arrows indicated the location of vesicles and the white lines indicate the cross-cutting lines for cross line analysis, scale bar: 10 μm. (A3-C3) Cross line analysis of the size of vesicles.

especially after the separation of vesicles from RBL-2H3 cells (Fig. 7(C)). And after the disintegration of these vesicles, a lot of granules could be observed on the substrate surrounding RBL-2H3 cells (Supplementary materials Fig. S 6). These results demonstrated the detailed morphological information of ionomycin-induced RBL-2H3 cell degranulation, which was dependent on the formation of a kind of peculiar vesicles to release granules. Previous studies by other high resolution microscopies have also demonstrated the emergence of vesicles during mast cell degranulation. Using transmission electron microscopy, García-Faroldi et al. (2010) showed the intracellular vesicle structures with micrometer sizes in mouse bone marrow derived mast cells. The intracellular vesicles were also observed by confocal microscopy in RBL-2H3 cells upon external stimulations (Xu *et al*., '98). These results demonstrated that the formation of vesicles was common features for mast cell degranulation, but we still could not confirm that the observed vesicles in this work were the same as or different from the vesicles previously reported. There were also lots of works indicated the granules during mast cell degranulation by scanning electron microscopy (Kimura *et al*., '98; Urb *et al*., 2009). But there were no reports about the vesicles during mast cell degranulation imaged by scanning electron microscopy, we supposed that these vesicles might be destroyed by the harmful sample procedures for scanning electron microscopy imaging.

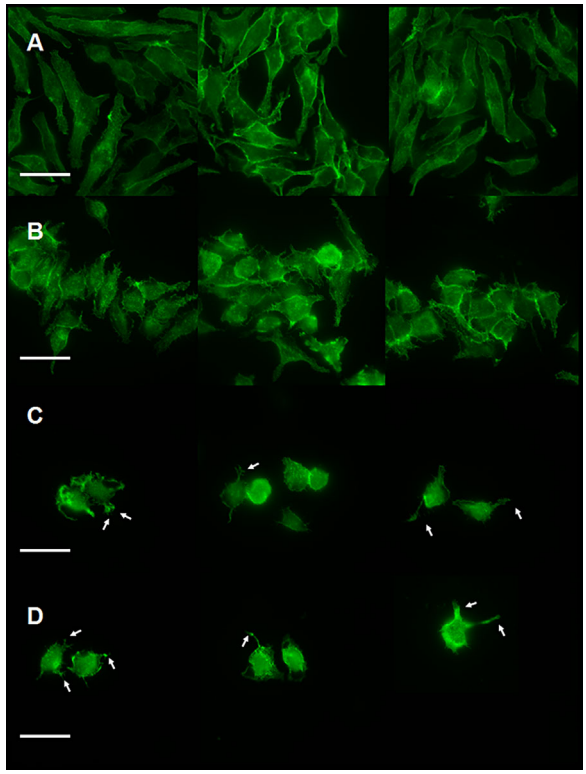

Fig 8. F-actin cytoskeleton structure of RBL-2H3 cells determined by fluorescence imaging. (A) Control RBL-2H3 cells. RBL-2H3 cells treated with ionomycin for (B) 5 min, (C) 10 min, and (D) 30 min, the white arrows indicate the formation of the unknown vesicles, scale bar: 50 μm.

Effects of Ionomycin on F-Actin Structure of RBL-2H3 Cells

As an intricate polymer network under cell membrane, the cytoskeleton of cells plays vital roles in maintaining the native morphology and function of cells, which therefore always shows changes associated with some important physiological phenomena of cells, such as apoptosis and inflammation (Starnes *et al*., 2014; Wei *et al*., 2015). And the underlying F-actin structure has been proved to play very important roles in mast cell activation (Deng *et al*., 2009). Fluorescence imaging was operated to demonstrate the alterations in F-actin structure of RBL-2H3 cells upon ionomycin stimulation, which would benefit our understanding of the roles of F-actin in ionomycin-induced degranulation of RBL-2H3 cells. As shown in Figure 8(A), control RBL-2H3 cells showed typical spindle shapes and uniform distributed F-actin in cells. After 5 min ionomycin stimulation, the spindle shaped RBL-2H3 cells presented contractive morphology (Fig. 8(B)), which was consistent with the results obtained by AFM imaging. The cell intensity of RBL-2H3 cells dramatically decreased after 10 min and 30 min ionomycin treatment (Fig. 8(C and D)). These fluorescence images also demonstrated the formation of a kind of peculiar vesicles after 10 min ionomycin stimulation (indicated by white arrows in Fig. 8(C)), which was also found in RBL-2H3 cells after 30 min ionomycin stimulation (indicated by white arrows in Fig. 8(D)). These vesicles were filled with F-actin and connected with RBL-2H3 cells by F-actin fibres, suggesting that F-actin must play very important roles in ionomycin-induced degranulation of RBL-2H3 cells. However, there were no vesicles or granules separated from the cells could be found by F-actin staining. These results implied that F-actin structure was involved in the early stage of vesicle formations. While after the disintegration of these vesicles, F-actin was destroyed and disappeared. Therefore, we proposed that F-actin might play important roles in maintaining the structure and function of these vesicles and the granules inside the vesicles would be released after the damage of F-actin structure.

Based on our results, the potential degranulation mechanisms of RBL-2H3 cells with or without ionomycin stimulation are summarized in Figure 9. Degranulation of control RBL-2H3 cells mainly happens in the cytoplasm area, which results in the emergence of granules and formation of pores on cell membrane. Similar degranulation processes of RBL-2H3 cells are also found in the early stage of

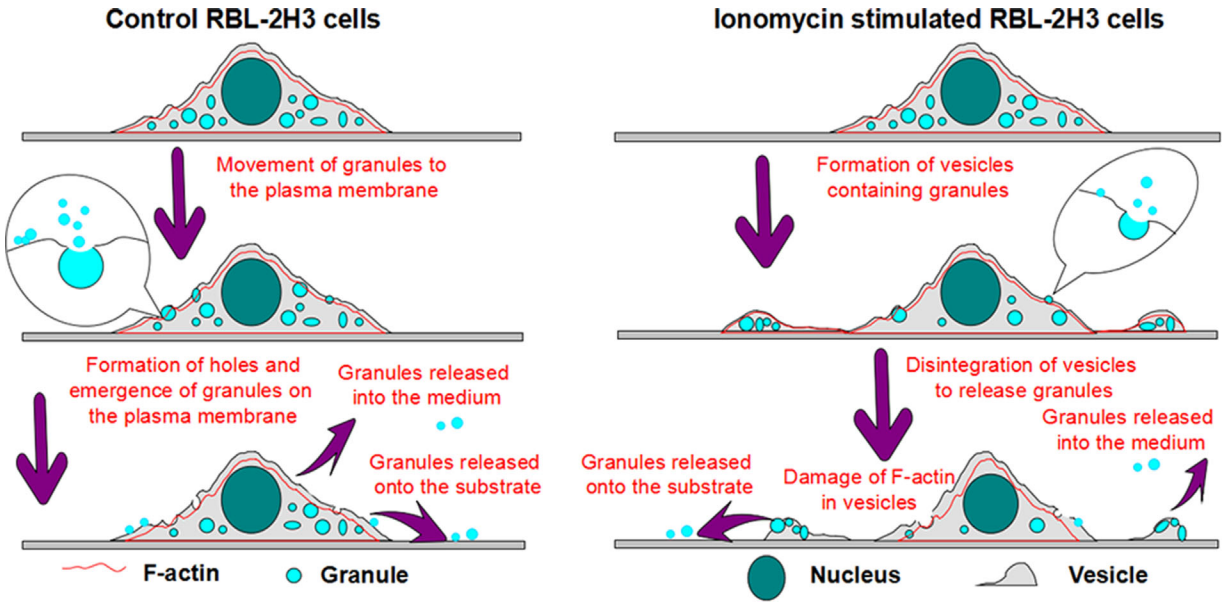

Fig 9. Schematic diagram of the two different degranulation mechanisms of control (left) and ionomycin-stimulated (right) RBL-2H3 cells.

ionomycin-stimulated RBL-2H3 cells. Moreover, a kind of different degranulation way is introduced in ionomycin-stimulated RBL-2H3 cells, which is associated with the formation of a kind of peculiar vesicles in the cytoplasm area of RBL-2H3 cells. The formed vesicles, which also contain F-actin skeleton inside them, are found to separate from the native cell body, but still connect with the native cell body through some structures containing F-actin. But after the damage of F-actin, these peculiar vesicles are found to undergo disintegration to release granules.

Conclusions

This work represents our initial effort to apply high resolution AFM for mast cell degranulation studies, which demonstrates the different degranulation mechanisms of control and ionomycin-stimulated RBL-2H3 cells. Ionomycin, a kind of calcium ionophore, is found to increase the calcium level and enhance the degranulation of RBL-2H3 cells. Ionomycin-induced RBL-2H3 cell degranulation is associated with the formation of a kind of peculiar vesicles in the cytoplasm area, which further separate from the native cell body and finally disintegrate to release granules by the controlling of F-actin. Our results suggest a different degranulation way of RBL-2H3 cells upon ionomycin stimulation using high resolution AFM imaging, which not only provides some important insights into ionomycin-induced mast cell degranulation, but also highlights AFM as a powerful tool for mast cell researches.

References

Baba Y, Nishida K, Fujii Y, et al. 2008. Essential function for the calcium sensor STIM1 in mast cell activation and anaphylactic responses. Nat Immunol 9(1):81–88.

Clapham DE. 2007. Calcium signaling. Cell 131(6):1047–1058.

Deng Z, Zink T, Chen HY, et al. 2009. Impact of actin rearrangement and degranulation on the membrane structure of primary mast cells: a combined atomic force and laser scanning confocal microscopy investigation. Biophys J 96(4):1629–1639.

Dupres V, Menozzi FD, Locht C, et al. 2005. Nanoscale mapping and functional analysis of individual adhesins on living bacteria. Nat Methods 2(7):515–520.

Frankel DJ, Pfeiffer JR, Surviladze Z, et al. 2006. Revealing the topography of cellular membrane domains by combined atomic force microscopy/fluorescence imaging. Biophys J 90(7):2404–2413.

García-Faroldi G, Rodriguez CE, Urdiales JL, et al. 2010. Polyamines are present in mast cell secretory granules and are important for granule homeostasis. PLoS ONE 5(11):e15071.

Giannone G, Ronde P, Gaire M, et al. 2004. Calcium rises locally trigger focal adhesion disassembly and enhance residency of focal adhesion kinase at focal adhesions. J Biol Chem 279(27):28715–28723.

Hong J, Aoyama S, Hirasawa N, et al. 2011. Suppression of intracellular calcium levels and inhibition of degranulation in RBL-2H3 mast cells by the sesquiterpene lactone parthenolide. Planta Med 77(3):252–U108.

Hu KK, Bruce MA, Butte MJ. 2014. Spatiotemporally and mechanically controlled triggering of mast cells using atomic force microscopy. Immunol Res 58(2–3):211–217.

Huang FH, Zhang XY, Zhang LY, et al. 2010. Mast cell degranulation induced by chlorogenic acid. Acta Pharmacol Sin 31(7):849–854.

Je IG, Choi HG, Kim HH, et al. 2015. Inhibitory effect of 1,2,4,5-tetramethoxybenzene on mast cell-mediated allergic inflammation through suppression of I kappa B kinase complex. Toxicol Appl Pharmacol 287(2):119–127.

Kemp SF, Lockey RF. 2002. Anaphylaxis: a review of causes and mechanisms. J Allergy Clin Immunol 110(3):341–348.

Kempuraj D, Madhappan B, Christodoulou S, et al. 2005. Flavonols inhibit proinflammatory mediator release, intracellular calcium ion levels and protein kinase C theta phosphorylation in human mast cells. Br J Pharmacol 145(7):934–944.

Kimura T, Andoh A, Fujiyama Y, Saotome T, Bamba T. 1998. A blockade of complement activation prevents rapid intestinal ischaemia-reperfusion injury by modulating mucosal mast cell degranulation in rats. Clin Exp Immunol 111(3):484–490.

Kraft S, Jouvin MH, Kulkarni N, et al. 2013. The Tetraspanin CD63 Is Required for Efficient IgE-Mediated Mast Cell Degranulation and Anaphylaxis. J Immunol 191(6): 2871–2878.

Lekka M, Laidler P. 2009. Applicability of AFM in cancer detection. Nat Nanotechnol 4(2):72; author reply 72–3.

Lenchner K, Grammer LC. 2003. A current review of idiopathic anaphylaxis. Curr Opin Allergy Clin Immunol 3(4):305–311.

Liu YP, Zeng L, Tian A, et al. 2012. EndoplasmicReticulum stress regulates the innate immunity critical transcription factor I RF3. J Immunol 189(9):4630–4639.

Mastuda H, Morikawa T, Ueda K, Managi H, Yoshikawa M. 2002. Structural requirements of flavonoids for inhibition of antigen-Induced degranulation, TNF-alpha and IL-4 production from RBL-2H3 cells. Bioorg Med Chem 10(10): 3123–3128.

Metcalfe DD, Peavy RD, Gilfillan AM. 2009. Mechanisms of mast cell signaling in anaphylaxis. J Allergy Clin Immunol 124(4):639–646; quiz 647–8.

Nakamura R, Nakanishi M. 1999. Atomic force microscopy to study the degranulation in rat peritoneal mast cells after activation. Immunol Lett 69(3):307–310.

Nakamura R, Nakanishi M. 2000. Atomic force microscopy to study the effects of ITIM-bearing FcgammaRIIB on the activation of RBL-2H3 cells. Immunol Lett 72(3):167–170.

Neher E. 1988. The influence of intracellular calcium concentration on degranulation of dialysed mast cells from rat peritoneum. J Physiol 395:193–214.

Ohashi T, Watanabe A, Nishigaki T, Azuma H. 1994. Electron microscopic studies on the inhibition of degranulation of rat mast cells by a novel anti-allergic agent, PTPC. Jpn J Pharmacol 66(1):7–16.

Ohshiro H, Suzuki R, Furuno T, Nakanishi M. 2000. Atomic force microscopy to study direct neurite-mast cell (RBL) communication in vitro. Immunol Lett 74(3):211–214.

Passante E, Ehrhardt C, Sheridan H, Frankish N. 2009. RBL-2H3 cells are an imprecise model for mast cell mediator release. Inflamm Res 58(9):611–618.

Passante E, Frankish N. 2009. The RBL-2H3 cell line: its provenance and suitability as a model for the mast cell. Inflamm Res 58(11):737–745.

Pi J, Jin H, Yang F, Chen ZW, Cai JY. 2014a. In situ single molecule imaging of cell membranes: linking basic nanotechniques to cell biology, immunology and medicine. Nanoscale 6(21):12229–12249.

Pi J, Li T, Liu JX, et al. 2014b. Detection of lipopolysaccharide induced inflammatory responses in R AW264. 7 macrophages using atomic force microscope. Micron 65:1–9.

Sampson HA, Munoz-Furlong A, Bock SA, et al. 2005. Symposium on the definition and management of anaphylaxis: summary report. J Allergy Clin Immunol 115(3): 584–591.

Schwartz LB, Austen KF, Wasserman SI. 1979. Immunologic release of beta-hexosaminidase and beta-glucuronidase from purified rat serosal mast cells. J Immunol 123(4):1445–1450.

Shumilina E, Lam RS, Wolbing F, et al. 2008. Blunted IgE-mediated activation of mast cells in mice lacking the Ca2+-activated K+ channel K(Ca) 3.1. J Immunol 180(12): 8040–8047.

Starnes TW, Bennin DA, Bing X, et al. 2014. The F-BAR protein PSTPIP1 controls extracellular matrix degradation and filopodia formation in macrophages. Blood 123(17): 2703–2714.

Stone KD, Prussin C, Metcalfe DD. 2010. IgE, mast cells, basophils, and eosinophils. J Allergy Clin Immunol 125(2 Suppl 2):S73–S80.

Urb M, Pouliot P, Gravelat FN, Olivier M, Sheppard DC. 2009. Aspergillus fumigatus induces immunoglobulin E-independent mast cell degranulation. J Infect Dis 200(3):464–472.

Wei L, Surma M, Gough G, et al. 2015. Dissecting the mechanisms of doxorubicin and oxidative stress-induced cytotoxicity: the involvement of actin cytoskeleton and RO CK1. PLoS ONE 10(7):e0131763.

Xu K, Williams RM, Holowka D, Baird B. 1998. Stimulated release of fluorescently labeled IgE fragments that efficiently accumulate in secretory granules after endocytosis in RBL-2H3 mast cells. J Cell Sci 111(Pt 16):2385–2396.

Yang W, Lee S, Lee J, Bae Y, Kim D. 2010. Silver nanoparticle-induced degranulation observed with quantitative phase microscopy. J Biomed Opt 15(4):045005.

Yang W, Schmid E, Nurbaeva MK, et al. 2014. Role of acid sphingomyelinase in the regulation of mast cell function. Clin Exp Allergy 44(1):79–90.

Zhang B, Alysandratos KD, Angelidou A, et al. 2011. Human mast cell degranulation and preformed TNF secretion require mitochondrial translocation to exocytosis sites: relevance to atopic dermatitis. J Allergy Clin Immunol 127(6):1522–31e8.

Supporting Information

Additional supporting information may be found in the online version of this article at the publisher's web-site.